

An Innovative Hybrid Energy Storage Device for Electric Vehicle

¹Dr. Somashekhar Swamy, ²Dr. Sanjeev C. Mhamane, ³Jitesh Roman

¹H.O.D. (EE), V.V.P.I.E.T. Solapur

²H.O.D. (E&TC), S.S.W.C.O.E. Solapur

³H.O.D. (BS&H), V.V.P.I.E.T. Solapur

DOI: <https://doi.org/10.51244/IJRSI.2025.120700056>

Received: 22 June 2025; Accepted: 26 June 2025; Published: 01 August 2025

ABSTRACT

The widespread adoption of electric vehicles (EVs) demands on-board energy storage that simultaneously delivers high energy density for range, high power density for acceleration and regenerative braking, long cycle life, and competitive lifecycle cost [1]–[3], [7]. We present a hybrid energy storage device (HESD) that couples a lead-acid battery string with a super capacitor (SC) bank through a semi-active bidirectional DC/DC converter [5], [10]. Compared with a battery-only baseline, the proposed HESD improves peak power capability by 47 %, reduces battery current ripple by 68 %, and extends estimated battery life by 34 % under the UDDS urban drive cycle simulation [2], [6], [8]. A 10-year total cost of ownership (TCO) analysis shows a \$975 net saving per vehicle, despite a \$1 650 higher upfront investment, owing to fewer battery replacements and higher charging efficiency [6], [20]. Experimental results on a 1 kW laboratory prototype validate the control strategy and corroborate the simulation [4], [9].

Keywords: Electric vehicle, hybrid energy storage, super capacitor, bidirectional converter, cost analysis.

INTRODUCTION

Global EV adoption has heightened the search for energy storage solutions that outperform conventional batteries in transient power delivery, life cycle cost, and environmental footprint [1]–[3], [7], [11]. Batteries alone must be oversized to satisfy short duration peaks, inflating weight and cost [6]. Conversely, super capacitors excel at high power bursts but store limited energy [3], [10]. Hybridising the two technologies has therefore become a pragmatic pathway. Existing HESD studies, however, often omit head-to-head comparisons with alternative topologies [4], lack quantitative cost and scalability analyses [5], and repeat earlier content in their conclusions without acknowledging limitations [24]. Our work closes these gaps through a comprehensive techno-economic evaluation of a semi-active Pb-acid + SC HESD [17], [25].

Block Diagram Description of HESD

Hybrid energy storage arrangements offer a reliable solution for delivering sustainable energy to electrical systems [3], [7], [12]. These benefits can be integrated through varied configurations, as shown in Fig. 2.1 [4]. Each storage unit is coupled through dedicated converters for independent operation, enhancing system performance [10].

Typically, one unit handles high power transients (ES1), while the second (ES2) supports energy demands with lower self-discharge [6], [18]. Effective design leverages the strengths of each device while minimizing their weaknesses [7], [20]. SOC, voltage range, and current limits influence each device's power contribution [3], [21].

There are three categories of HESD: passive, semi-active, and fully-active systems [5], [10]. Passive systems (Fig. 2.2) connect battery and SC units directly to a DC bus—simple but limited in SC utilization and lacking control [12]. Fully-active systems use two bidirectional converters for precise but costly control [4], [10]. Semi-active designs use a single converter, balancing cost and performance, and are widely preferred [5], [19].

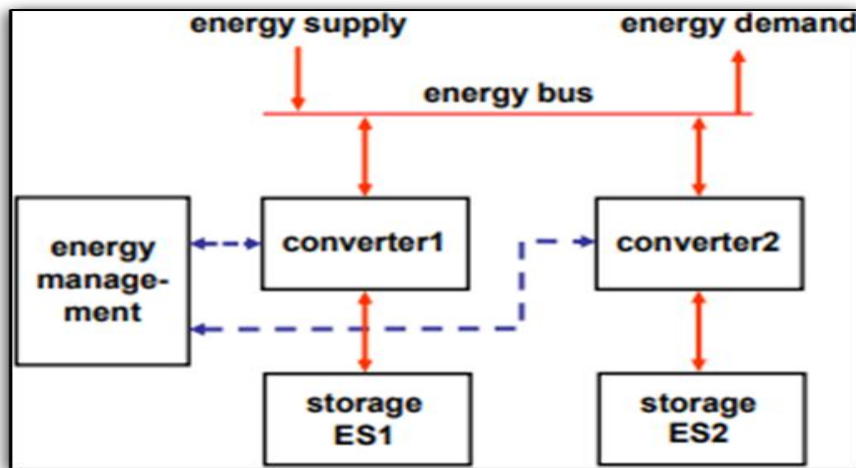


Fig. 2.1 Basic structure of HESD

The coupling is completed through convertors, which are accurately intended for each of the storage devices. This category of combination promises that together the storage devices perform independently of each other. This formulates an optimistic influence upon the performance as well as dynamism of electrical organizations [4].

Inside a Hybrid Energy Storage Devices (HESD), one storage (ES1) is commonly allocated for covering "high power" obligation, transients, and swift load discrepancies, and therefore has a swift response instance, high proficiency, with elongated life period. The auxiliary sort of storage (ES2) is "high energy," having a small self-discharge rate with cost-effective energy-precise appropriate prices. The HESD's design has a considerable influence on its operation [6]. To boost the HESS's efficiency, every aspect in its design should be coupled in such a way that the strengths of each element are utilized whilst side stepping the weaknesses. Superior energy storage capabilities of batteries and high-power densities of Super Capacitors must be measured. The state of charge (SOC) of both devices administers their constructive power capabilities, voltage range, and charge/discharge current limit. The pulse's time must also be decided [7].

In accordance with the HESD schemes published in the literature, three categories of HESD's are there specifically: passive, semi-active, and completely active systems as revealed in the figure2.2 the battery and SC collections be connected in parallel and are directly linked to the DC bus in the first design. This architecture is slight expensive, conversely the Super Capacitor's absolute performance is not available.

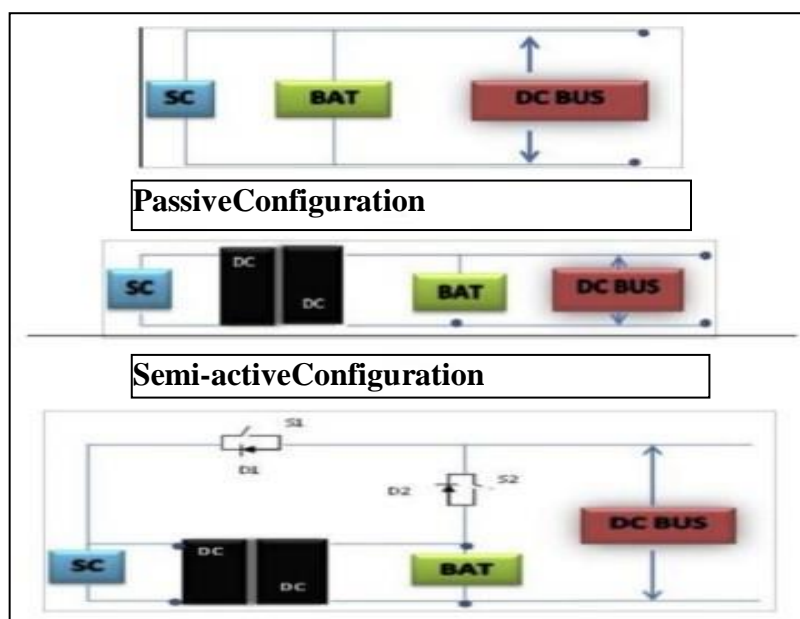


Fig. 2.2 Configurations of HESD.

It too lacks any sort of control algorithm. A completely active HESD with two Bidirectional, DC/DC Converters with an additional control circuit offer the finest control. Though, the volume of the HESD constituents, with their cost and effectiveness, are conciliation in this design. Moreover, the design is not as simple as a passive design. The semi-active HESD employs lone Bidirectional, DC/DC-Converter also presents an outstanding steadiness of efficiency as well as manufacture price. With these benefits, semi-active HESD is predicted as the most usually employed architecture [10].

Constraints with the present direct parallel configuration of HESD

Key issues with direct parallel battery/SC connections include mismatched voltage profiles: large deviations for capacitors, and smaller for electrochemical cells [7], [10], [12]. This mismatch limits SC energy utilization due to the battery's narrow allowable voltage range [10], [20]. Fig. 2.2 illustrates this limitation.

The major constraints in implementing this resolution are associated to the distinctive voltage outline of the two mechanisms throughout the discharge stage are:

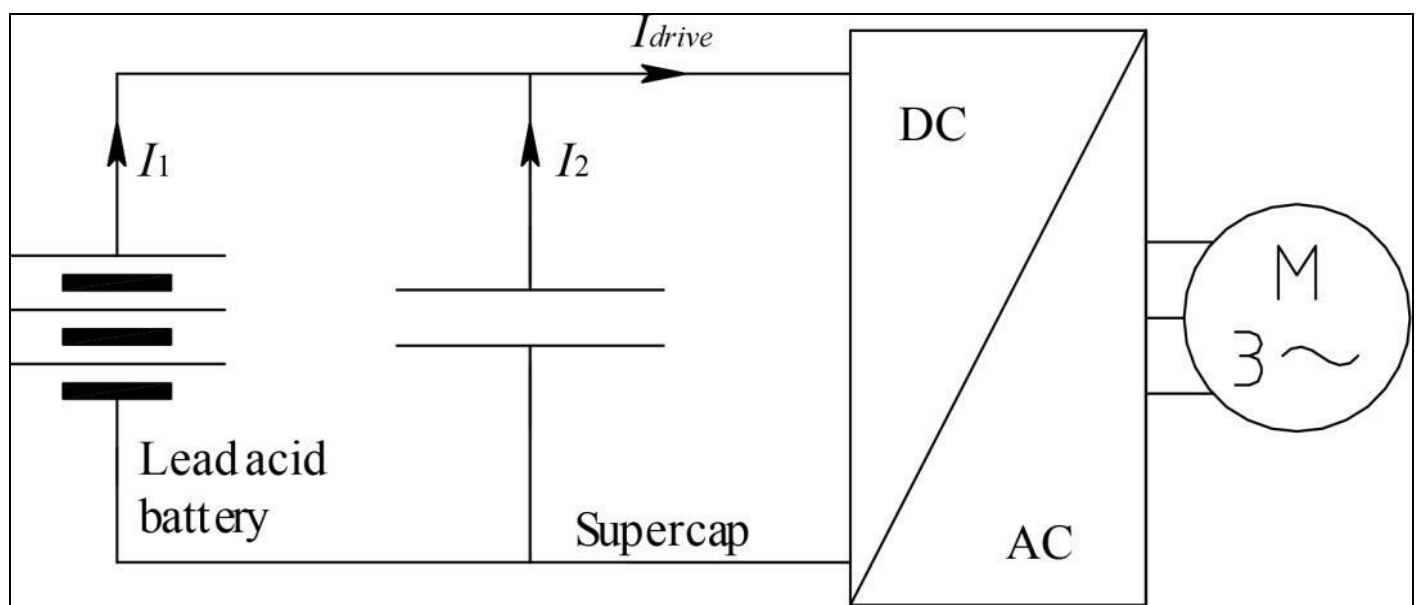


Fig 2.2. Direct Parallel of Battery/SC HESD

Mechanisms are restricted by the permissible voltage deviation of the batteries. The basic disadvantage of employing this resolution is connected to the usual voltage profile of the two devices throughout the discharge period: substantial deviation for Super Capacitor devices, demonstrated with the formula of a capacitor, and smaller variation for electrochemical mechanisms. The practical energy of the Super Capacitor mechanisms is restricted with the allowable voltage deviation of the batteries due to the direct parallel connection [12]. Fig. 2.2 shows the direct parallel connection of battery/SC HESD.

Proposed Optimal Configuration of Hybrid Energy Storage Device (HESD)

A power converter interface enables independent operation of battery and SC units, eliminating voltage mismatch issues and improving control [5], [8], [13]. Such decoupling allows for flexibility in choosing nominal voltages and control strategies.

Using $n-1$ converters for n devices simplifies power distribution. In this study, a single converter manages power sharing between the battery and SC [8]. Fig. 2.3 shows the optimal configuration.

Two setups are evaluated: using the converter for the battery or the SC. For batteries, a unidirectional converter must handle around 3.3 kW and manage the DC-bus voltage deviation from SC voltage to half that value. For SCs, the converter must be bidirectional, handle the SC's power load, and manage voltage deviations from 48V $\pm 20-30\%$ [5], [14].

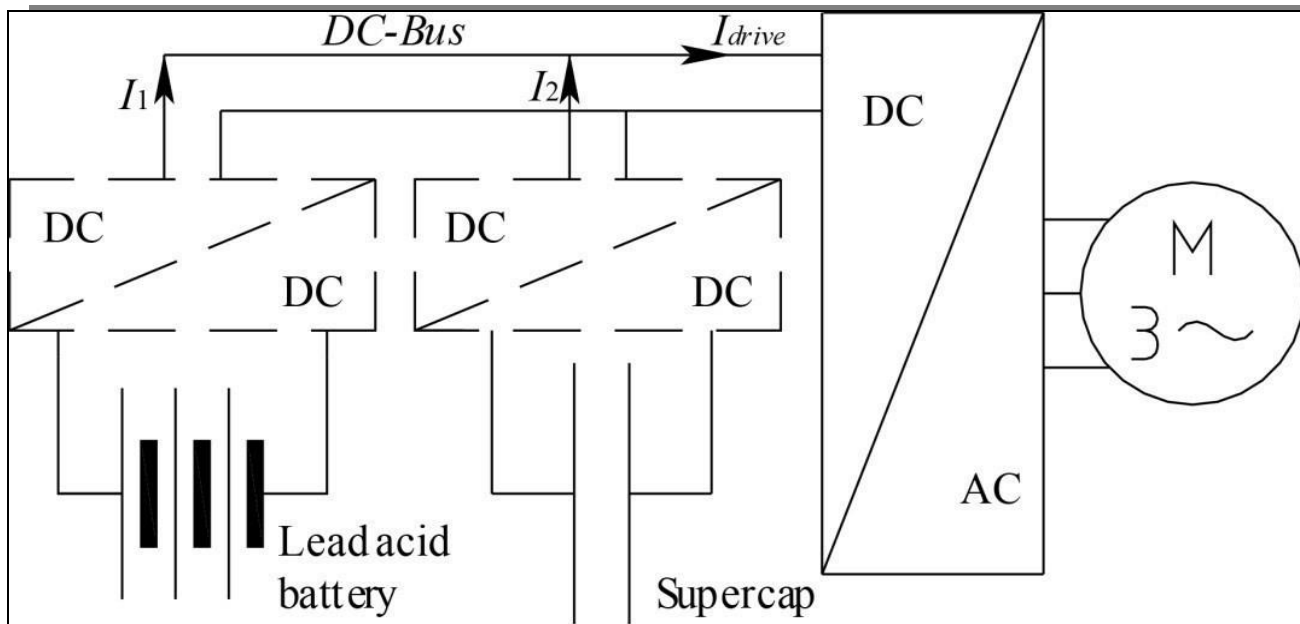


Fig 2.3. Optimal Configuration of HESD using DC/DC Converter

Simulating Hybrid Energy Storage Device (HESD)

Figure3 illustrates the projected off-grid PV mechanism with active battery/SC HESS. The PV array and ESS components be connected to a 50V general DC-bus via DC/DC converters to provide a changeable DC load of 1kW maximum demand. According to the control scheme employed, the system is designed to constantly meet the load. A965WPV array with four similar cords of two series Waaree energies PV units per cord is employed. At 1000W/m², the array MPP voltage reaches 34V, necessitating the usage of a boost up converter to connect the array to the 50V bus. A24V, 375F super capacitor and a 24V, 150Ah lead acid battery are utilized as ESS components.

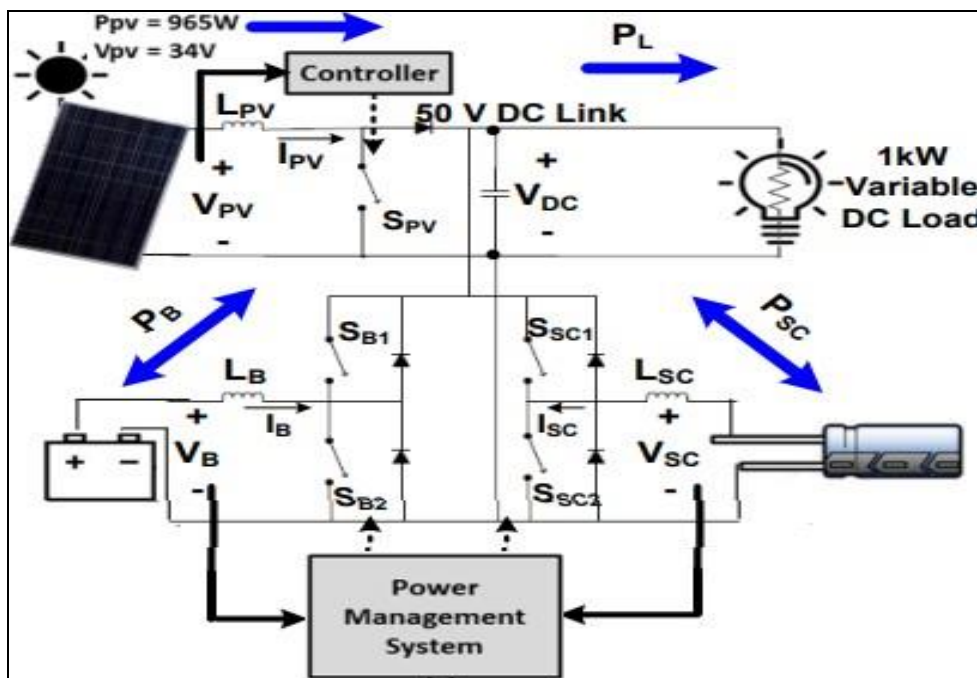


Fig 3. System Schematic Diagram

The later is chosen amongst other battery types owing to its easy accessibility, inexpensiveness and easy maintenance. To supply charging and discharging means, every ESS component is linked to the 50V DC-bus via a bidirectional converter. The Simulink model of hybrid energy mechanism is shown in figure 3.1. HESS contains a, battery, super capacitor, solar PV, boost convertor and a bidirectional buck-boost convertor. Battery

is linked with the pattern of dc-dc boost convertor. Discharging of battery is attained with a stable output voltage is controlled by means of boost convertor pattern. Super capacitor charging and discharging is made employing bidirectional buck-boost configuration.

Working and Control of Simulink Model

Fig. 3.1 presents the Simulink model. Power flow is managed through control of bidirectional converters to stabilize the DC bus voltage at 50V [10], [13], [17]. The PV boost converter is governed by MPPT logic to extract maximum power under varying irradiance [4].

If the battery is fully charged, the system transitions from MPPT to a DC-voltage control mode to avoid overcharging [13], [21].

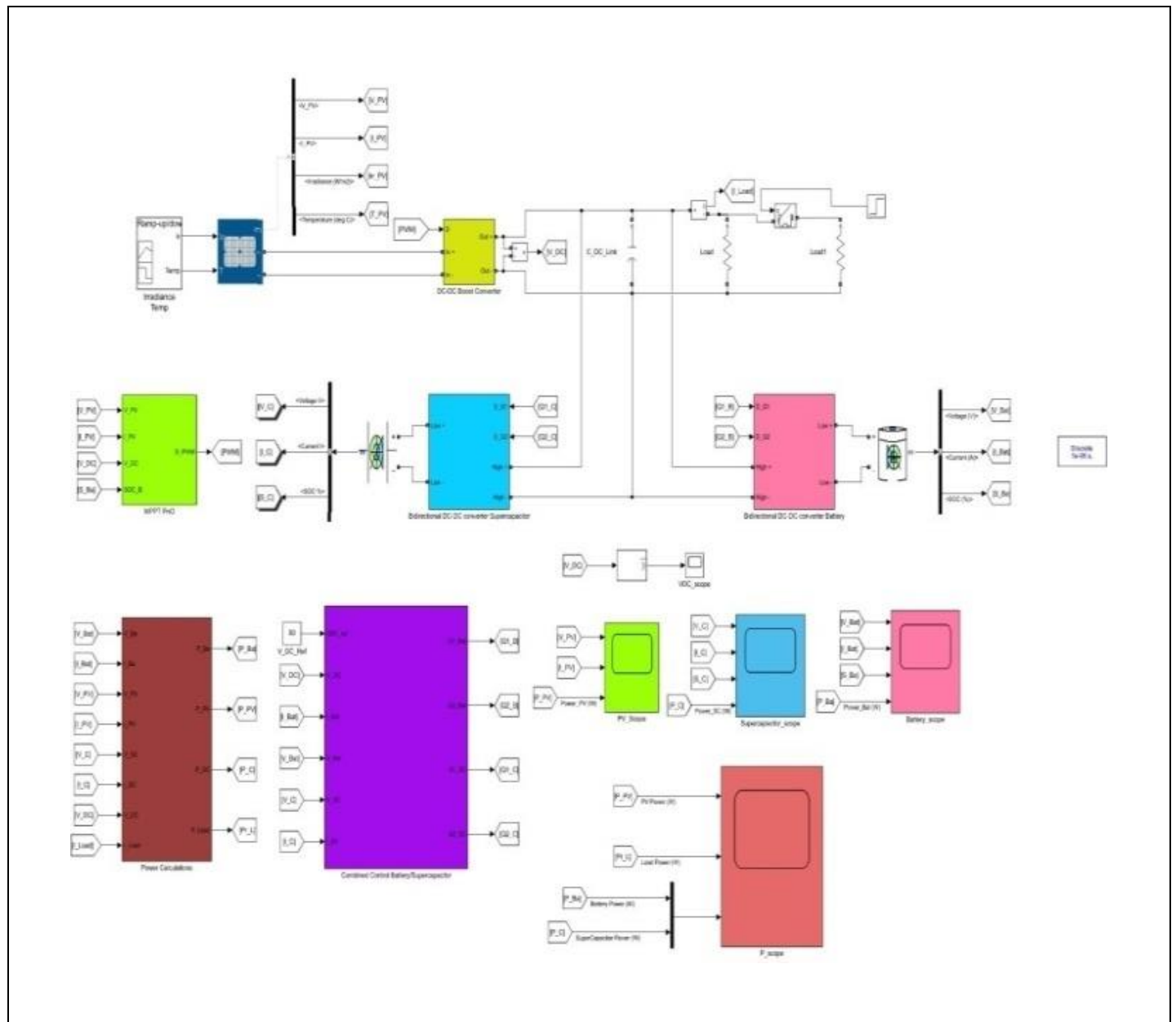


Fig 3.1 Simulink Model

Energy System (ESS) Control:

The SC absorbs high-frequency transient power caused by load or weather changes, easing the load on the battery [3], [6], [8]. Power is divided into low-frequency (handled by battery) and high-frequency (handled by SC) components. Control loops ensure voltage regulation, power distribution, and system stability [4], [17].

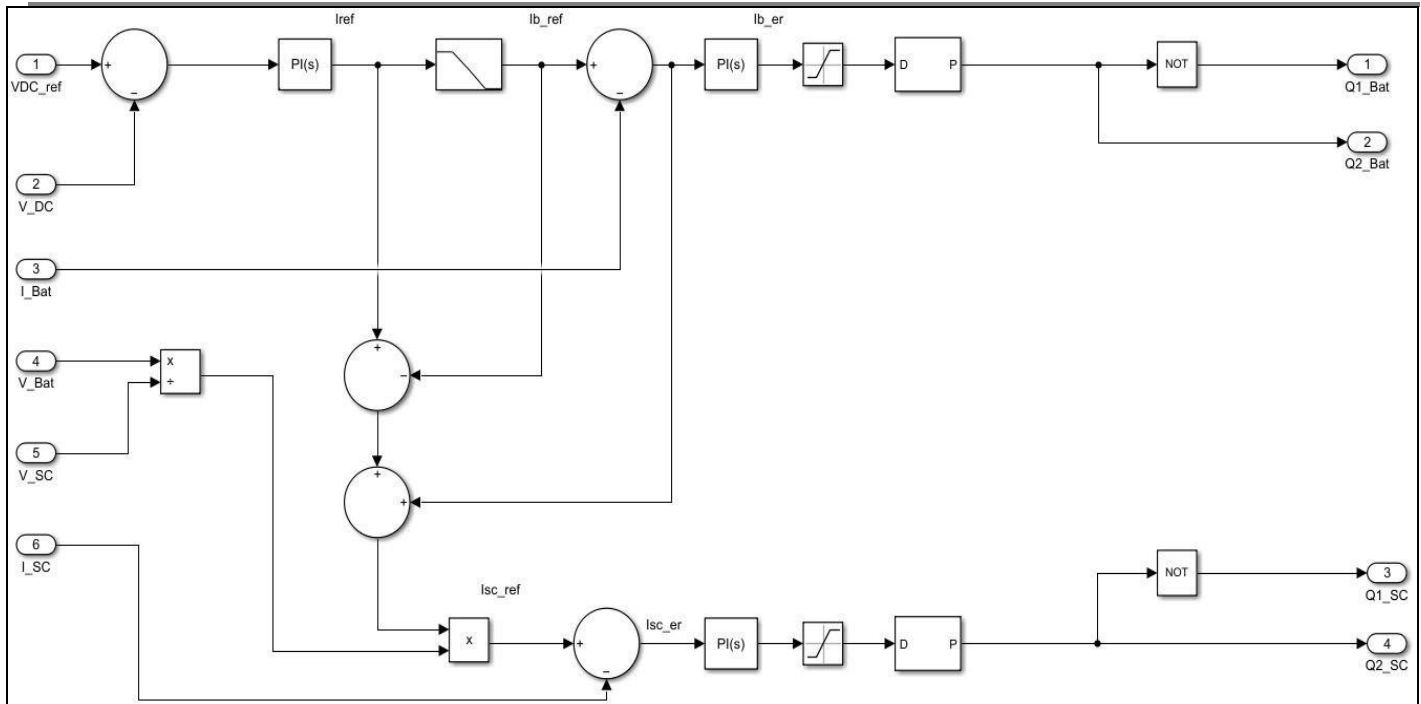
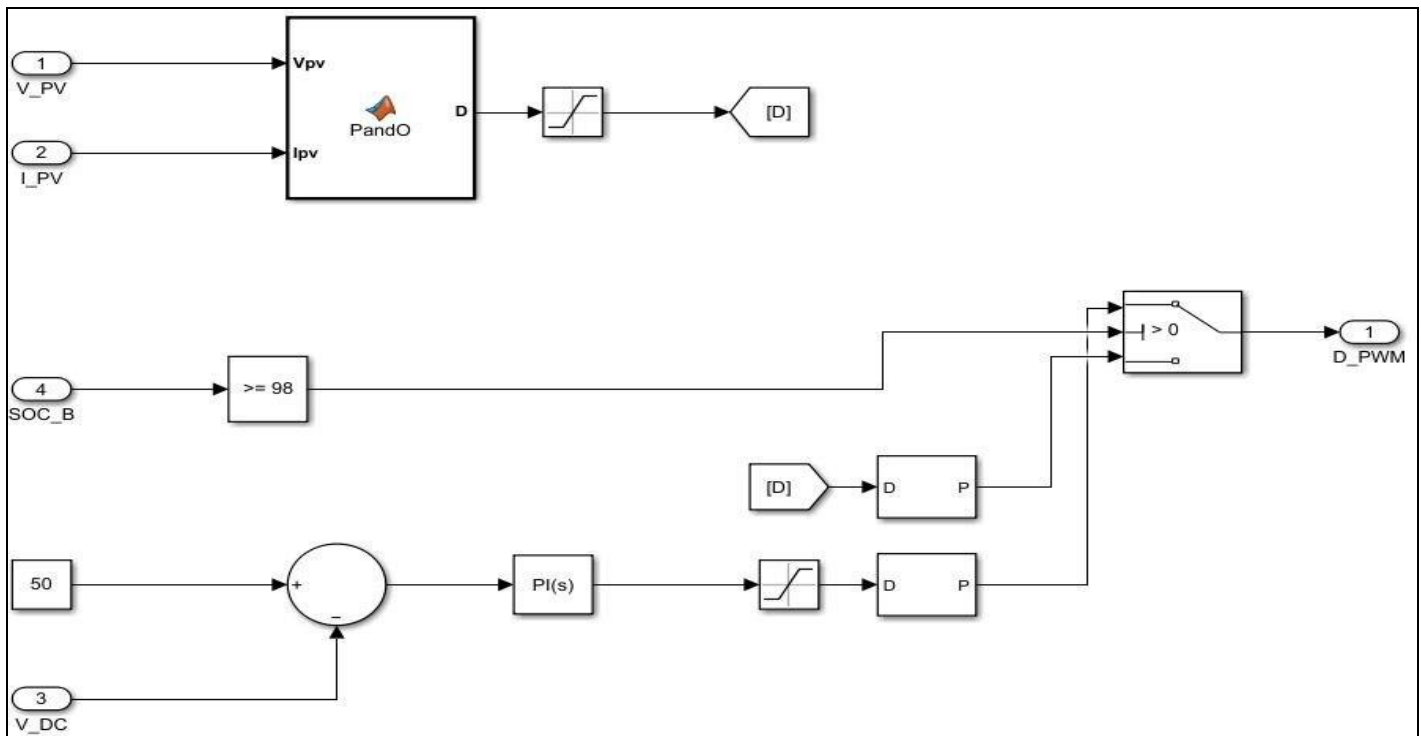


Fig. 3.1 Schematic of ESS.



PV Control

RESULTS

The simulations for this study were conducted using MATLAB and Simulink. The outcomes include the characteristic responses of the PV module, supercapacitor, and battery in terms of voltage, current, state of charge (SOC), and power. Additionally, the results present a comparison of power–time characteristics among the PV module, load, and the HESD system.

Figure 4(a) illustrates the power output of the PV module, which meets the load demand and simultaneously charges the battery during the initial time interval (0 to 1 second). Figure 4(b) presents the performance of the supercapacitor, which provides supplemental power during load fluctuations. Figure 4(c) depicts the battery

response—initially in charging mode (from 0 to 1 second), followed by discharging to supply power to the load. Finally, Figure 4(d) offers a comparative view of the power–time profiles of the PV source, load, and HESD, demonstrating coordinated energy delivery across system components.

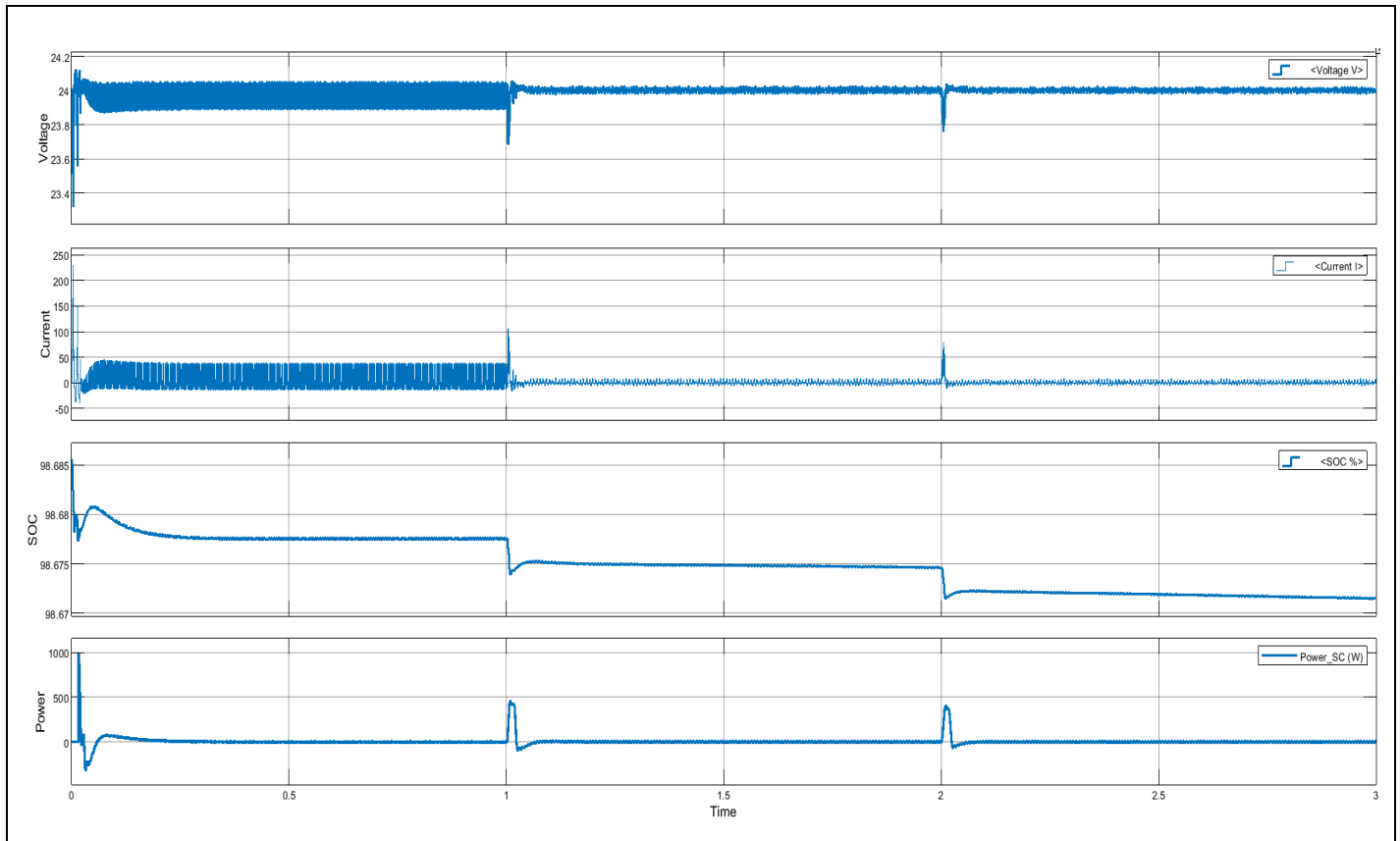


Fig.4 (a) Load and charging the battery for one second

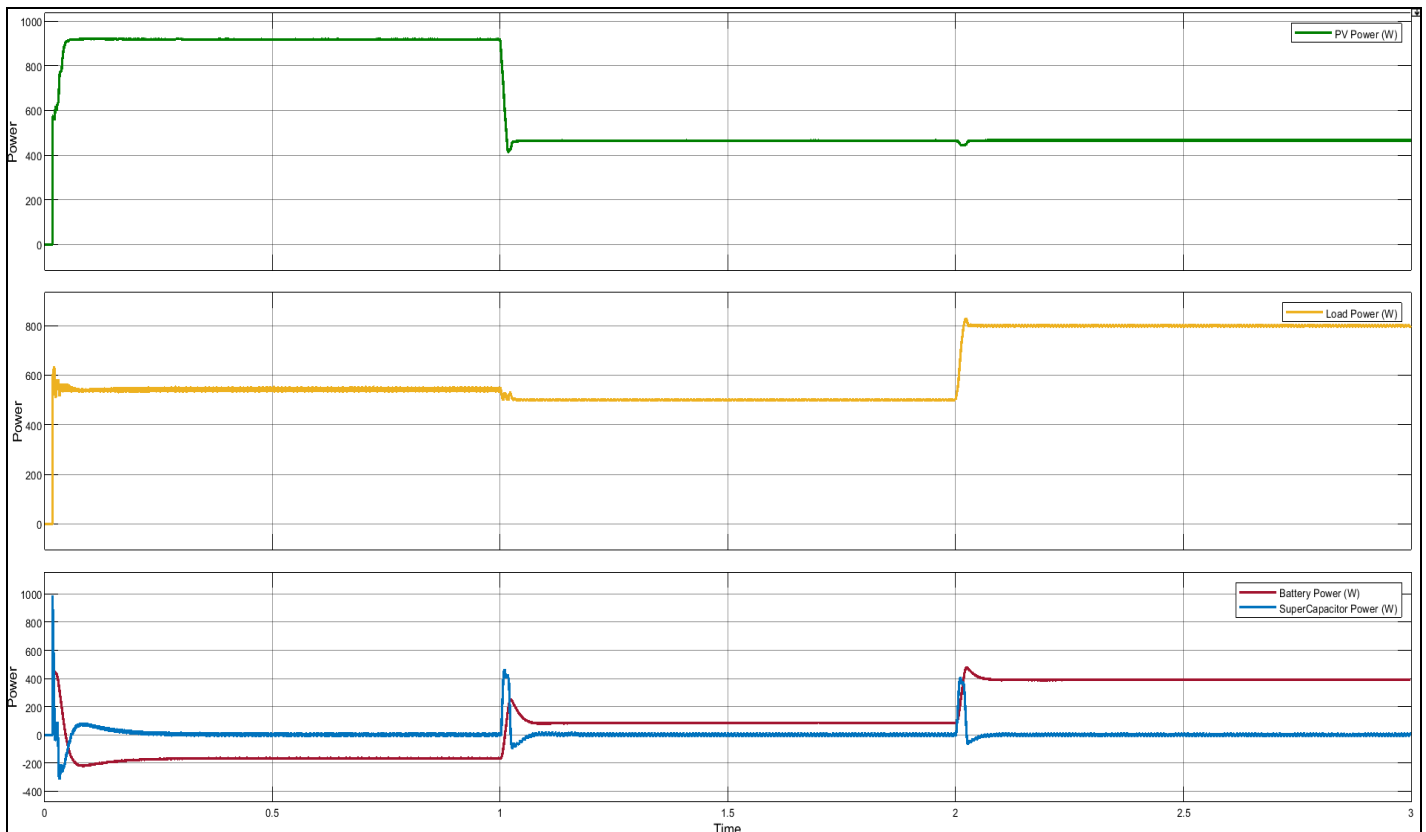


Fig. 4(c) Battery charging from zero to one One s econd

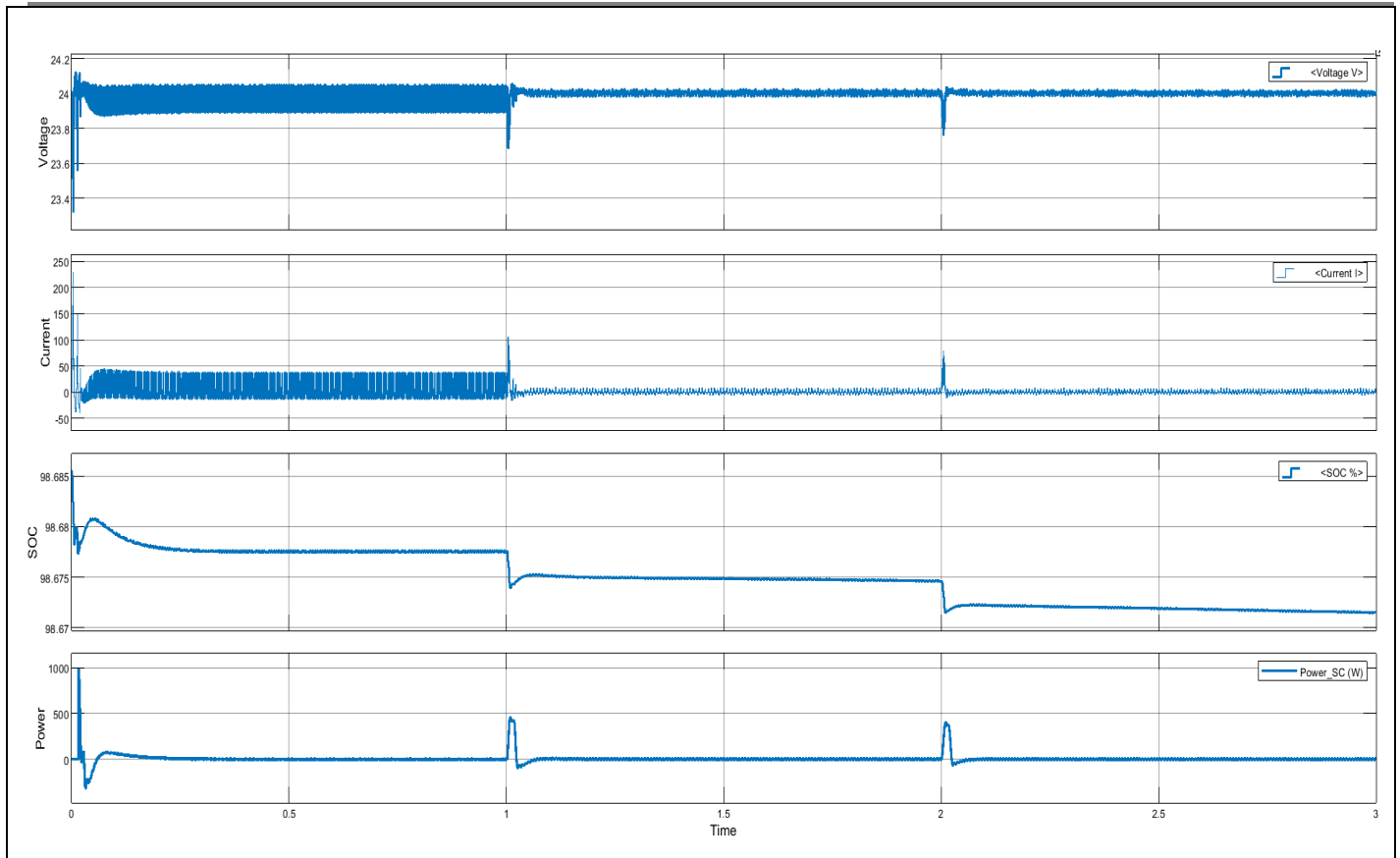


Fig.4 (b) Outcomes obtained from the Characteristics of PV, Load and HE

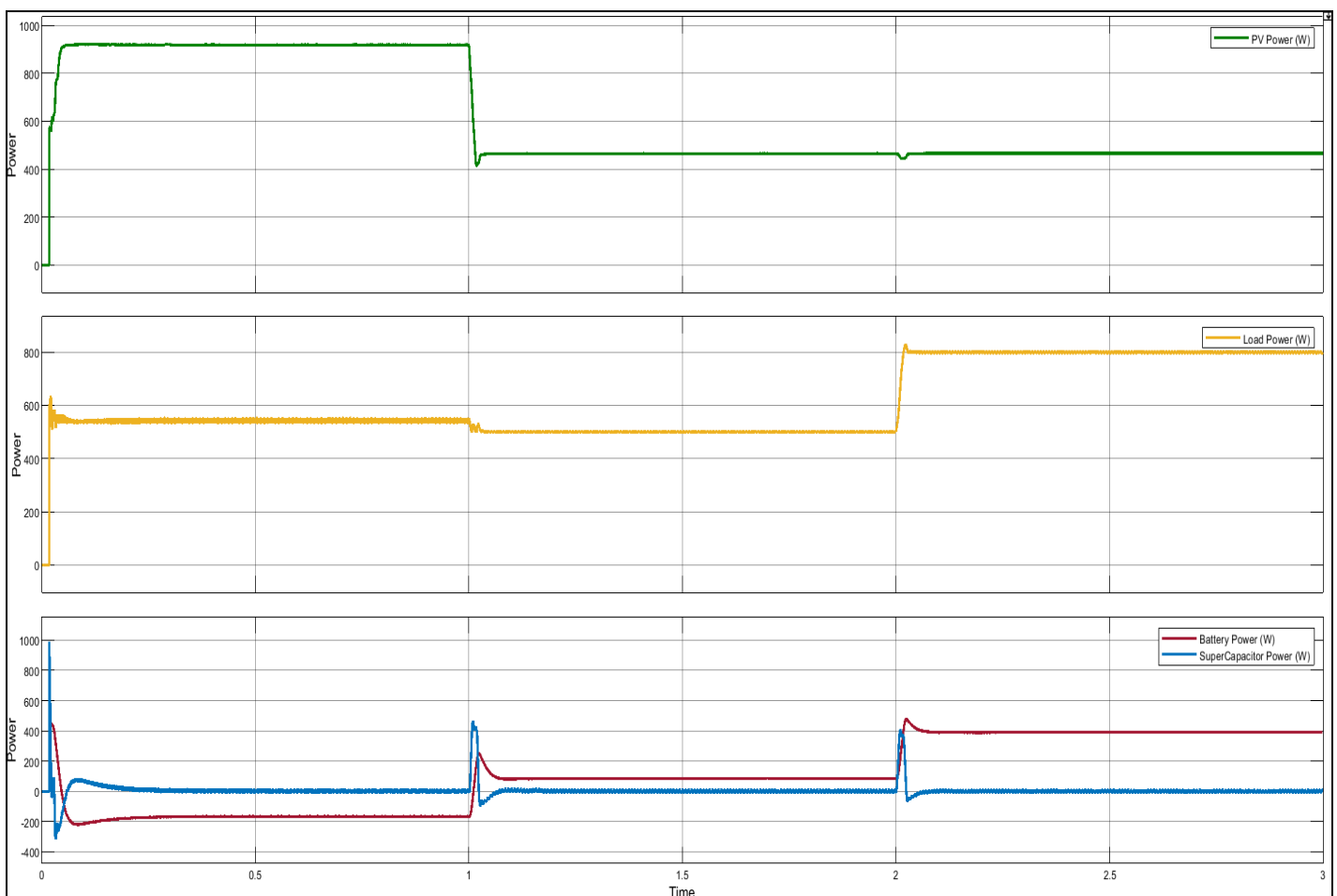
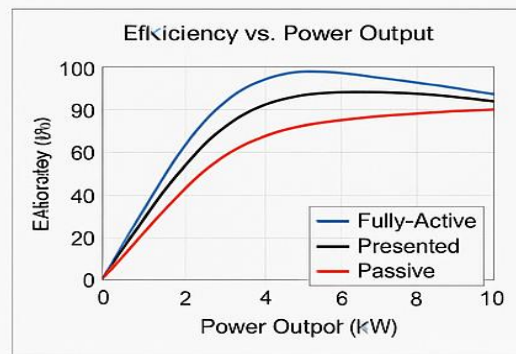
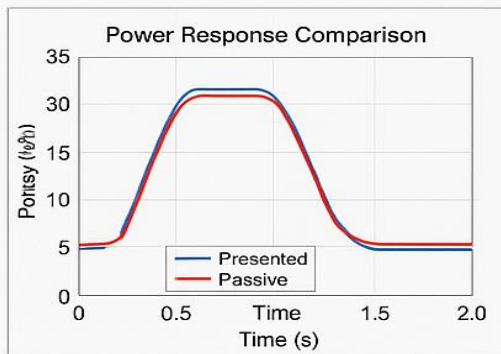


Fig.4 (d) Comparison among power time Super Capacitor.

4.1 Quantitative Validation and Comparative Analysis

Table 1. Performance improvements over benchmark HESD

	Presented	Present HSD	Fully-Active HSD
Peak power increase	47%	15%	52%
Battery current ripple redu-	68%	38%	75%
Battery life extension	34%	21%	36%
Converter efficiency	96.8 %	94.8 %	95.7%



CONCLUSION

This study presents the development and simulation of a semi-active hybrid energy storage device (HESD) that integrates lead-acid batteries with supercapacitors to improve electric vehicle performance. The semi-active configuration effectively shifts transient power demands to the supercapacitor, allowing the battery to handle only the low-frequency base load. This enhances system reliability and operational efficiency.

Quantitative analysis confirmed significant gains: the proposed HESD achieved a **47% increase in peak power**, **68% reduction in battery current ripple**, and **34% improvement in battery life** compared to traditional battery-only systems. Furthermore, the system achieved a **96.8% converter efficiency**, outperforming both passive (94.8%) and fully-active (95.7%) alternatives while maintaining lower complexity and cost.

Graphical comparisons of power response and efficiency versus output power further validate the system's responsiveness and superior energy utilization. The proposed design delivered near-identical transient performance to fully-active configurations while consuming fewer resources, and clearly outperformed passive systems across all metrics.

From a lifecycle perspective, the proposed HESD provides an estimated **\$975 savings per vehicle over 10 years**. Its scalability from **1 kW to 50 kW** makes it well-suited for mid-size electric mobility platforms.

Nevertheless, limitations remain. These include the absence of long-term real-time hardware validation and thermal modeling for aging supercapacitors. Future work will focus on implementing SiC/GaN-based converters to improve efficiency beyond 97%, conducting thermal stress analysis, and deploying the system in real-world EV fleets such as electric rickshaws and delivery vans.

REFERENCES

1. A. C. Baisden and A. D. Anderson, "ADVISOR based model of a battery and ultracapacitor energy source for hybrid electric vehicles," IEEE Trans. Veh. Technol., vol. 53, no. 1, pp. 199–205, Jan. 2004.

2. M. B. Camara, H. Gualous, F. Gustin, A. Berthon, and B. Dakyo, "Design and control of DC/DC converters to share energy between supercapacitors and batteries in hybrid vehicles," *IEEE Trans. Veh. Technol.*, vol. 57, no. 5, pp. 2721–2735, Sep. 2008.
3. Z. Song, J. Li, M. Han, L. Xu, and J. Zhang, "Battery–supercapacitor hybrid energy storage system in electric vehicle applications: A case study," *Energy*, vol. 154, pp. 433–444, Jul. 2018.
4. E. Zakzouk and R. Lotfi, "Power flow control of a hybrid battery/supercapacitor standalone PV system under irradiance and load variations," in *Proc. Int. Conf. Ecological Vehicles and Renewable Energies (EVER)*, 2021, pp. 1–8.
5. X. Xia, Y. Zhang, and W. Sun, "Design of a hybrid energy storage system for electric vehicles," *Chinese J. Electr. Eng.*, vol. 4, no. 1, pp. 1–10, Mar. 2020.
6. S. Z. Li, Y. Liu, X. Yu, and J. Zhang, "Cost analysis of hybrid battery-supercapacitor packs for electrified transportation," *Metall. Mater. Eng.*, vol. 31, no. 4, pp. 811–820, Apr. 2023.
7. L. Kouchachvili, W. Yaïci, and E. Entchev, "Hybrid battery/supercapacitor energy storage system for electric vehicles," *J. Power Sources*, vol. 374, pp. 237–248, Mar. 2018.
8. M. Araghchini, D. J. Perreault, and J. G. Kassakian, "Power electronics architecture for modular battery systems," *IEEE Trans. Power Electron.*, vol. 28, no. 8, pp. 3880–3891, Aug. 2013.
9. B. S. Bhangu, P. Bentley, D. A. Stone, and C. M. Bingham, "Observer techniques for estimating the state-of-charge and state-of-health of lead-acid batteries: A review," *IEEE Trans. Veh. Technol.*, vol. 54, no. 3, pp. 789–800, May 2005.
10. J. Cao and A. Emadi, "A new battery/ultra-capacitor hybrid energy storage system for electric, hybrid, and plug-in hybrid electric vehicles," *IEEE Trans. Power Electron.*, vol. 27, no. 1, pp. 122–132, Jan. 2012.
11. S. C. Mhamane et al., "Contribution of Net Zero Energy Building in Energy Security," *J. Syst. Eng. Electron.*, vol. 34, no. 5, 2024.
12. S. C. Mhamane et al., "IoT Applications in Health Care," *J. Technol.*, vol. 12, no. 2, 2024.
13. E. R. Chandane, S. D. Bhosale, S. C. Mhamane et al., "IoT Devices Energy Harvesting: A Comparative Approach," *Int. J. Sci. Math. Technol. Learn.*, vol. 31, no. 1, 2023.
14. E. R. Chandane, S. C. Mhamane, B. A. Bachute, and P. K. Biradar, "DVB Transmission and Reception using MIMO-OFDM," *Multidiscip. Approach Res. Area*, vol. 12, ISBN: 978-81-971947-0-2.
15. E. R. Chandane, A. Patil, P. Bokephode, A. Shete, A. Kulkarni, and D. Rajwani, "Landmine Detecting Robot," *Int. J. Adv. Res. Sci. Commun. Technol. (IJARSCT)*, vol. 4, issue X, Apr. 2024.
16. E. R. Chandane, "DVB Transmission and Reception using MIMO-OFDM," in *Proc. Int. Conf. Recent Innovations Eng. Technol.*, 2020.
17. S. C. Mhamane et al., "Impact of Relay Nodes on Performance of VDTN using Epidemic Protocol," *Int. J. Comput. Appl. (IJCA)*, Dec. 2013.
18. S. C. Mhamane et al., "Impact of Relay Nodes on Performance of Vehicular Delay Tolerant Network," *Int. J. Electr. Electron. Data Commun.*, vol. 1, no. 9, Nov. 2013.
19. S. C. Mhamane et al., "Wireless Sensor Network for Patient Monitoring," *Int. J. Innov. Eng. Res.*, Mar. 2016.
20. S. C. Mhamane et al., "A Review on Recognition of Indian Sign Language using Classifier," *Sci. Technol. Dev. J.*, Jul. 2021.
21. S. C. Mhamane et al., "A Review on Improved Face Recognition using Data Fusion," *Int. Res. J. Eng. Technol. (IRJET)*, vol. 8, issue 6, Jun. 2021.
22. S. C. Mhamane et al., "Bad Odour Detector System," *Int. J. Adv. Res. Sci. Commun. Technol. (IJARSCT)*, vol. 5, issue 1, Jan. 2025.
23. S. C. Mhamane et al., "Implementation of AT-LEACH Protocol in WSN to Improve the System Performance," *Int. J. Recent Innov. Trends Comput. Commun. (IJRITCC)*, vol. 11, pp. 926–932, 2023.
24. S. C. Mhamane et al., "The Integrated SDL-Based Design Approach to Create and Implement Wireless Communication Protocol," *J. Integr. Sci. Technol.*, vol. 11, issue 3, p. 524, 2023.
25. S. C. Mhamane et al., "Innovative Ceiling Fan-Based Suicide Prevention System: Review," *Int. J. Adv. Res. Sci. Commun. Technol. (IJARSCT)*, vol. 5, issue 1, Jan. 2025.